Cite this article
Vaghasia BM, Rachchh NV, Mehta A, Paramasivam P and Ayanie AG (2025) Biomimetic nacre-inspired composites reinforced with glass fibers for enhanced strength. *Bioinspired, Biomimetic and Nanobiomaterials* **14(4)**: 177–193, https://doi.org/10.1680/jbibn.25.00017

Research Article
Paper 2500017
Received 23/04/2025; Accepted 24/09/2025

Bioinspired, Biomimetic and Nanobiomaterials

Biomimetic nacre-inspired composites reinforced with glass fibers for enhanced strength

B.M. Vaghasia
Department of Mechanical Engineering, Marwadi University, Rajkot, India

N.V. Rachchh
Department of Mechanical Engineering, Marwadi University, Rajkot, India

Ankush Mehta
Department of Mechanical Engineering, Faculty of Engineering & Technology, Marwadi University Research Centre, Marwadi University, Rajkot, India

Prabhu Paramasivam
Department of Research and Innovation, Saveetha School of Engineering, SIMATS, Chennai, India

Abinet Gosaye Ayanie
Department of Mechanical Engineering, Adama Science and Technology University, Adama, Ethiopia (corresponding author: abinet.gosaye@astu.edu.et)

This study explores enhancing the mechanical properties of fiber-reinforced polymer composites using a biomimetic approach inspired by nacre. Composites were fabricated with hexagonal glass fiber platelets cut via high-precision laser, embedded in a polyester resin matrix. Ten specimens were produced with varying platelet sizes (10–30 mm) and interplatelet gaps (2–6 mm), arranged in three laminate layers with a 0°/45°/90° stacking sequence. Mechanical testing revealed that larger platelets improved tensile strength, hardness, and density, while wider interplatelet gaps reduced performance. The optimal configuration, with 25 mm platelets, showed an 18% increase in impact strength (1.9 J/m → 2.3 J/m) and a 115% increase in flexural strength (59 MPa → 127 MPa) compared to monolithic laminates. Fourier transform infrared spectroscopy analysis indicated variations in resin curing and fiber–matrix interactions, and X-ray diffraction patterns showed changes in crystallinity and residual stress. Scanning electron microscopy imaging confirmed reduced delamination and enhanced crack resistance in biomimetic laminates. These findings demonstrate that nacre-inspired glass fiber composites exhibit significantly improved mechanical behavior, highlighting their potential for engineering applications, including automotive crash components and protective headgear.

Keywords: biomaterials/biomimetic materials/glass fiber platelets/interplatelet spacing/mechanical characterization/nacre-inspired composites

1. Introduction

The living organism has long been a foundation of motivation for engineering structure, mostly in the advancement composite material.[1] One specific natural design that has gathered significant attention is nacre, generally known as mother of pearl, a natural composite material found in inner layer of mollusk shells having exceptional toughness and strength, which is obtained to its hierarchical structure composed of brittle aragonite platelets and a soft organic protein matrix.[2] This unique combination of stiff platelets and a compliant matrix has motivated researchers to replicate these bioinspired structures in synthetic composites to improve their mechanical properties.[3–5] Bioinspired composites address remarkable mechanical strength under extreme environmental conditions and demonstrating high toughness and stiffness in high pressure environment, possess good thermal stability at elevated temperatures, and resistance against chemical degradation.[1–5] Natural nacre material contains significant crushing strength,[6] having multilayered lamellar architecture,[7] contains biopolymer linkage with excellent interfacial strength,[8] possessing structural and mechanical properties used in various application like Velcro, Al_2O_3-PMMA (aluminum oxide, poly-methyl-methacrylate),[9] and combination of natural ceramic and biopolymer constituent.[10] The architecture of the lamellar structure of mollusk shell have been identified over different length scales[11–13] from numerous characterization tech-niques, including scanning electron microscopy (SEM), transmission electron microscopy (TEM), atomic force microscopy (AFM), and Fourier transform infrared spectroscopy (FTIR). Gebremaryam *et al.*[14] explored the utilization of Teff seed coat powder act as a bio-filler reinforcement in epoxy composites which demonstrating significant enhancement in mechanical properties and thermal stability, with an optimum composition 7.5% Teff powder composite leads to promising percentage of bio-filler which is suitable for structural applications. Shahapurkar *et al.*[15] investigated the embedding of Habeshian short banana fiber in epoxy matrix core which is sandwiched between woven banana fiber composite that demonstrating improvement of tensile, compressive, and fracture toughness properties with optimal value of 10 wt.% fiber content reflect the significant improvement of mechanical properties for structural applications.

Nacre-inspired designs have been progressively used in different types of composite materials, including ceramic/polymer composites having dental CAD/CAM application,[16] carbon fiber-based ceramic composite,[17] Al-based metal matrix composites,[18–20] graphene-based composites,[21–23] and polymer matrix composites.[24–26] These designs mimic the hierarchical structure of

natural nacre, leading to significant enhancements in mechanical properties such as strength,[18] toughness,[19] and flexibility. In addition, they improve tribological behavior, offering superior wear resistance and reduced friction.[20] The microstructural features of nacre-inspired composites also contribute to enhanced radiation resistance, making them suitable for applications in extreme environments.[22] Moreover, these materials demonstrate shape memory properties, further broadening their potential applications in advanced engineering and smart material systems.[23]

Nacre-based carbon fiber composite is fabricated using vat photopolymerization process with the effects of various fillers on flexural properties being examined and molecular dynamics simulations used for study of atomic structure and filler interactions within the nacre scaffold. But the high cost of the fabrication process and time are still challenging aspects; moreover, the only flexural property is analyzed; it required characterization of other properties like tensile strength, impact strength, and so on for broader characterization.[17] Ji *et al*.[27] fabricated nacre-inspired composite having aramid papers with a 'brick-and-mortar' structure and combination of 3D aramid nanofiber (ANF) matrix and 2D carbonylated basalt nanosheets (CBSNs) as fillers material. It provides remarkable mechanical and electrical properties. Nacre like ceramic-polymer composites with different orientation of architectures and its effect on compression fatigue strength are observed. This study reveals that fatigue strength is improved by hindering the crack propagation through crack deflection due to different orientation of brick-and-mortar and lamellar structure.[28] Review of different natural materials having good mechanical properties like nacre, shrimp shell, conch shell, horns, hooves, and beetle wings inspired composite material fabricated through multi-material additive manufacturing process.[29] Study of nacre-inspired brick and mortar structure and its value of fracture strength 1700–3000 times higher than single constituent aragonite material.[30] The effect of the hierarchical structure of nacre in mechanical properties like tensile strength and shear strength observed by Lin and Meyers.[31] Low velocity impact strength of bioinspired composite like dactyl clubs of mantis shrimp like material for enhancement of damage tolerance capability studied.[32] Patel and Adalja[33] investigated the dynamic performance of a glass fiber based rotating composite shaft through experimental and FEM analysis which gives a significance of laminate composite in dynamic properties and application. In addition, bioinspired mechanism implemented in various filed like medicine for protecting blood cell membren,[34] electronics equipment design,[35] cleaner and absorber improvement,[36] photocatalyst application,[37,38] organ implant,[39] milling process optimization,[40,41] antibacterial drug system,[42] and biomedical implant design.[43]

Based on above literature, the bioinspired material having great potential for developing advanced composite material having capability to improve the mechanical and dynamic strength of material under different loading condition. Majority of work mainly depend on high-cost manufacturing process like multi-material additive manufacturing process; high-cost reinforcement fiber material like (carbon fiber, aramid fiber and graphene etc.) leads to the reduction scalability of bioinspired material in real-world utilization. So, this research work explores the low-cost fabrication process like E-glass fiber reinforcement material and GP LR grade resin as matrix material and mechanical characterization of nacre-inspired composites, which focused on the influence of biomimic platelet size and interplatelet spacing on the mechanical properties of bioinspired composite material. By using hexagonal-shaped glass fiber platelets as reinforcements within a polyester resin matrix, the impact and flexural strength of composite material was improved. The values of the impact strength and flexural strength improved by 18% and 46%, respectively. The study focuses on effect of different platelet dimensions and their distribution on tensile strength, flexural strength, hardness, density, and impact resistance.

2. Material and methods

Nacre like three layered glass fiber chopped strand matt (CSM) form with 350 GSM (grams per square meter) used as a reinforcement material, LR grade (laminated resin) polyester resin used as a matrix material to mimic bonding part of nacre. Laminate prepared through simple hand layup technique in open molding process environment having dimension 300 × 300 mm and thickness 3 mm maintained to fulfill ASTM standard requirement for evaluating mechanical and physical properties. Hand lay-up process is applicable for large-scale composite production through its low initial investment, flexibility in manufacturing large and complex shapes, and increasing scalability through employing large manpower and workstations suitable for dense population countries. This hand layup method is widely employed in industries involved in the fabrication of manholes and chemical containers, where achieving cost-effective production at medium scale. A total of ten bio-inspired laminates were prepared, of which the first five were fabricated with a uniform platelet gap, while the biomimetic platelet size varied from 10 mm to 30 mm. Similar way another five biomimetic laminate prepared with the same platelet size variation with change in gap between biomimetic platelet like 2 and 6 mm. Figure 1 shows the hierarchical architecture of biomimetic laminate having three distinct layers with each layer plantlets

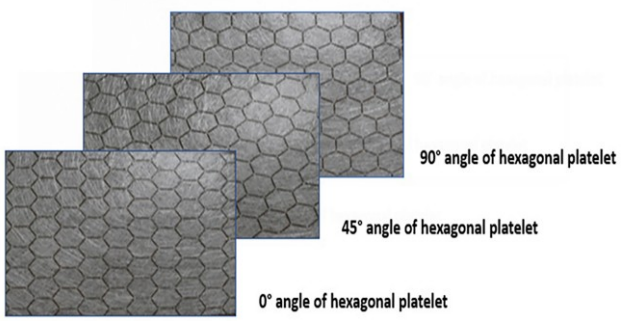

Figure 1. Biomimetic platelet orientation of three different layers of laminate

are arranged at angle of 0°/45°/90° to mimic nacre like lamellar brick-and-mortar structure. Fabrication of biomimetic platelet with different size, gap, and orientation is obtained through laser cutting process with accuracy 0.01 mm. All three layered biomimetic reinforcement material with LR grade polyester resin as a matrix material makes laminate thickness 3 mm through hand lay-up process. Figure 2 represents a hexagonal platelet with a side length fixed to 10 mm and a thickness of 1 mm engraved by CO_2 gas laser cutting machine. The cutting process was performed with process parameters like a cutting speed of 7 mm/min and a cutting mode operation. Initially, a computerized drafting model was constructed with varying side length and thickness, which acts as an input for the laser cutting machine to generate cutting path on reinforcement.

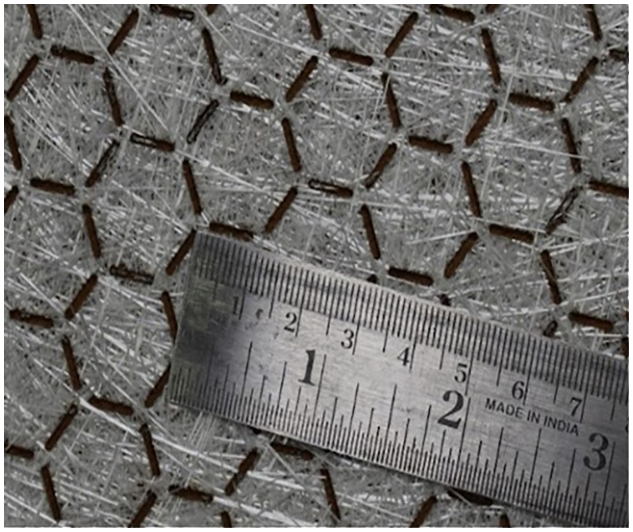

Figure 2. Hexagonal platelet with side length 10 mm

2.1 Nacre-inspired biomimetic reinforcement and matrix material

Figure 3 shows the arrangement of nacre like platelet with varying hexagonal side length like 10, 15, 20, 25, and 30 mm and gap between platelet is fixed at 1 mm maintained through automated highly precision laser cutting machine. The fabrication of different platelet sizes reveals the influence of size of platelets in mechanical and impact performance of biomimic composite laminate over plain non-biomimic laminate. Low-cost E-glass fiber chopped strand matt is used to mimic the nacre like platelets material.

Figure 4 reveals the biomimetic platelet with varying gap like 2, 3, 4, 5, and 6 mm obtained through same laser cutting process. Figures 2 and 3 represent the single layer of reinforcement with zero-degree platelet orientation and rest of the other two layer arranged at 45° and 90°, respectively. Total ten laminate fabricated to find effect of biomimetic platelet size and gap distribution. Biomimetic platelet with different size provides the stiffness and gap between platelet filled with resin material provides the required softness for overall laminate. Combination stiffness and softness lead to lighter and tougher laminate for required mechanical application.

Laminated resin (LR) grade polyester is used for matrix material and it is also used for filling gap between two platelets. It mimics as a mineral bridge function in overall laminate structure.

2.2 Fabrication of biomimic nacre like laminate

Total ten laminates with variation of platelets size and interplatelet placing are processed through low-cost hand layup method performed with help of rigid and highly finish flat mold surfaces as a base for processing by cleaning of molding surface with 70 grade fine stone grinding paper to remove leftover particles, cure resin dumps, and maintain uniform surface finish. After surface preparation surface coating is applied through petroleum wax material

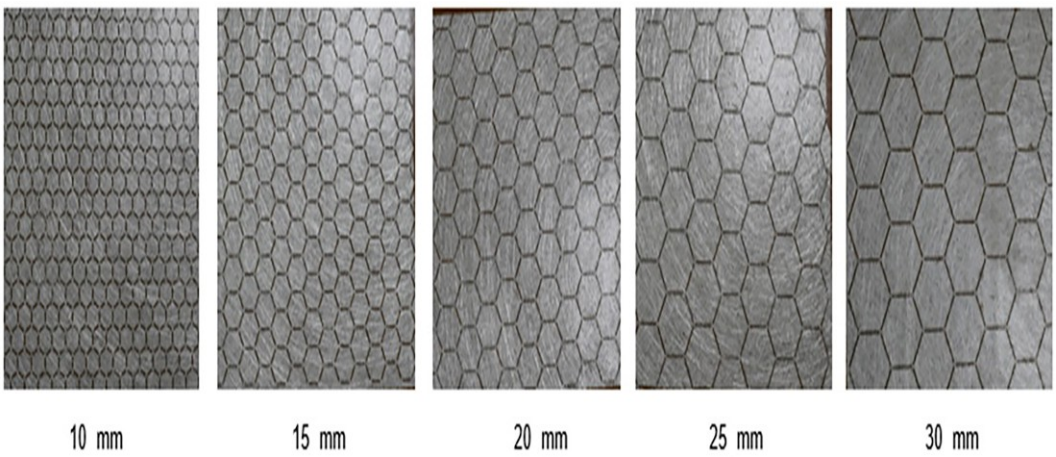

Figure 3. Biomimetic platelet sizes (10–30 mm) with fixed 1 mm gap

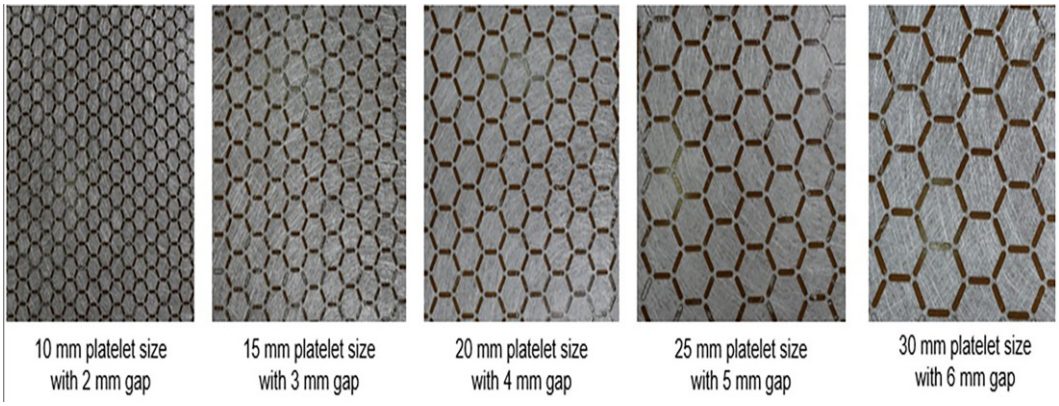

Figure 4. Biomimetic platelet with varying gap (2–6 mm)

which acts as mold release agent after curing process. Allowing wax to dry for 10 min after that the lamination work is carried out at normal room temperature and pressure. The total weight of cobalt and hardener was determined as 1% of the total weight of laminated-grade resin used to fabricate the laminates with E-glass fiber reinforcement. Air bubble interruption is removed with help of manual roller pressing. After that allowing bioinspired laminates to cure at room temperature for 48-h time duration and then raw samples with dimension 300 × 300 × 3 mm were released from mold surface with help of chisel tool. Standard shape and size of specimen for different mechanical test were cut as per ASTM D638 for testing tensile properties, ASTM D790 for evaluating bending property and ASTM D256 used for Izod impact test strength measurement. Hardness of specimen is directly measured from raw sample size through barcol indenter as per ASTM D2583 standard. For density measurement, samples were cut as per size of platform 20 × 20 mm of hydrometer.

2.3 Fabrication of non-biomimetic laminate (monolithic (plain) laminate)

Stacking of total three layers of glass fiber CSM sheet with 350 GSM having size 300 × 300 mm used as reinforcement material, while in matrix material configuration: GP resin LR grade with mixing of 1 percentage hardener and 1 percentage cobalt by weight of LR resin used for fabrication of monolithic material laminate which is non-biomimetic and its property compare with nacre-inspired biomimetic composite laminate.

2.4 Testing of biomimic nacre like laminate

2.4.1 Tensile test

Tensile test in uniaxial manner is performed as per ASTM D638[44–48] standard. Figure 5 shows the sample attachment in Universal testing machine with capacity 1000 kN and displacement rate 5 mm/min. Extensometer is attached to specimen for measurement of strain within the elastic limit. The test is conducted on different sizes of nacre like platelet 10, 15, 20, and 30 mm size and variation of interplatelet spacing 2, 3, 4, 5, and

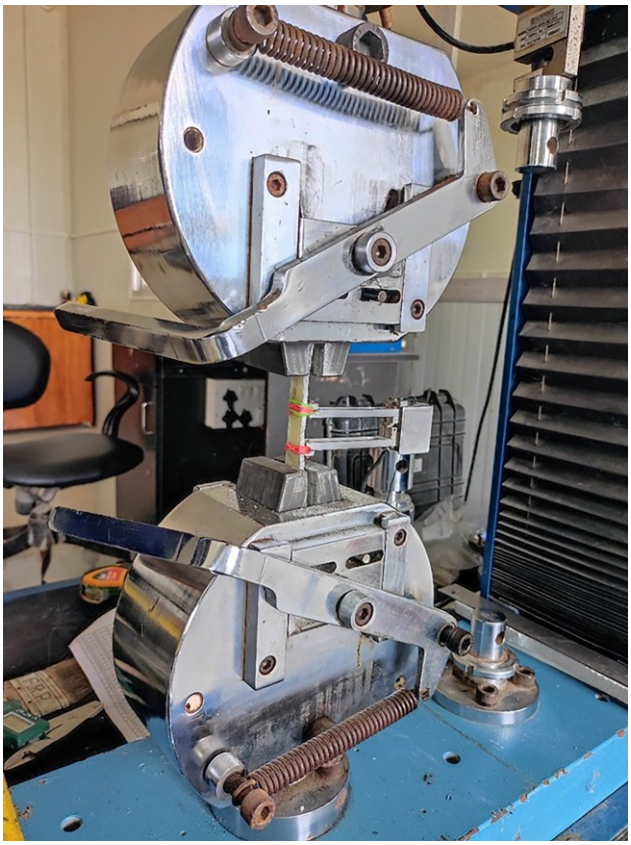

Figure 5. Specimen attachment with extensometer arrangement

6 mm and also non-biomimetic monolithic sample with same thickness 3 mm and geometry tested. All biomimic and non-biomimic laminate specimen contains smooth vertical side and having constant cross-section geometry at gauge section gradual increase with beveled shaped grips located at its end's specimen geometry having following configuration (length × width × thickness) 165 × 19 × 3 mm maintained (refer to Figure 6) which represent the dog bone shaped specimen.

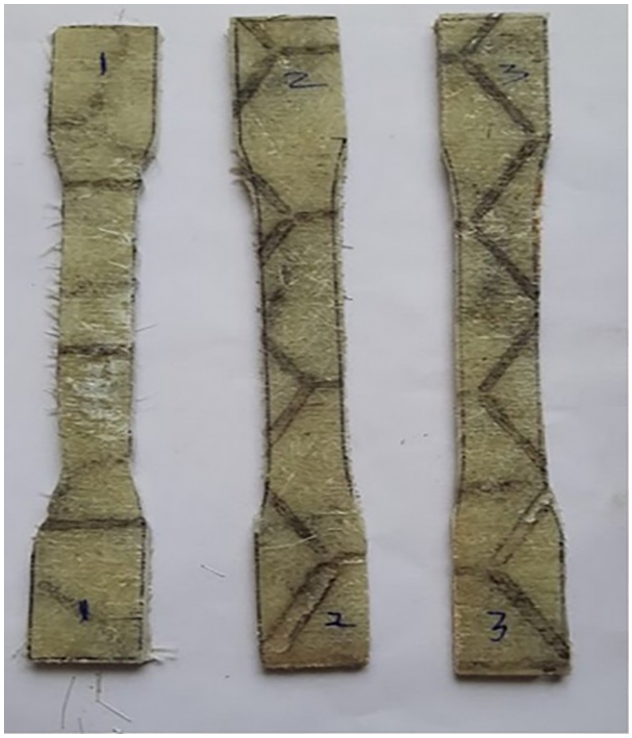

Figure 6. Bioinspired dog bone specimen

2.4.2 Flexural test

In this test findings flexural properties like flexural strength and flexural modulus of nacre like biomimetic composite laminate are obtained through static flexural testing as per ASTM D790[49–53] standard all specimen fabricated in rectangular-shaped geometry which is clearly illustrated in Figure 7 having following configuration 70 × 12 × 3 mm maintained. All arrangement like sample arrangement and position of roller support grip are mentioned in Figure 8. The flexural specimen is

Figure 7. Flexural testing specimen

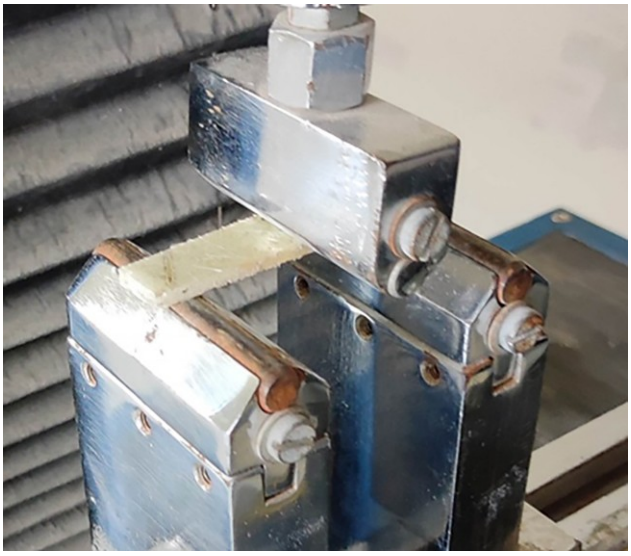

Figure 8. Specimen subjected to three point bending in UTM apparatus

placed between two roller supports with span length 48 mm in UTM with recommended testing speed of 2 mm/min maintained.

2.4.3 Impact test

The energy absorption-dissipation capacity, impact resistance, and fracture resistance of a material can be obtained from the Izod impact. In addition, it gives the information about the nature of material in terms of combination of brittle and ductile region. Figure 9 shows the impact testing apparatus with notched sample held between the fixture subject to following machine parameters: impact load 24 J and speed 3.6 m/s, specimen geometry having following configuration 50 mm (length) × 30 mm (width) × 3 mm (thickness) maintained. Impact tester of IT504 Plastic Impact (Tinius Olsen, USA) is used to perform impact test with hammer of 41.25 N force and specimen notched tip radius of 1 mm used to fulfil the standard requirement. Testing machine and specimen arrangement maintained as per ASTM D256[54–58] requirement. All test specimen were conditioned like finishing edges of samples with fine emery paper, and specimen maintained at standard room temperature and so on; specimen geometry, Izod impact tester machine with display unit is shown in Figure 10.

2.4.4 Hardness test

The surface hardness of bioinspired laminate is obtained by adopting ASTM D2583 standard procedure which reflects the Barcol hardness value of all class of glass fiber reinforcement polymer matrix composite material. Total 11 specimens with 40 mm × 40 mm dimension with thickness 3 mm were indented through barcol indenter. All cured bioinspired nacre like laminate specimens were kept in normal atmospheric condition for 48 h time duration before testing. The hardness test is then conducted in the laboratory at ambient atmospheric conditions. Five indentation marks are placed on different location of

Figure 9. Samples with notched shape

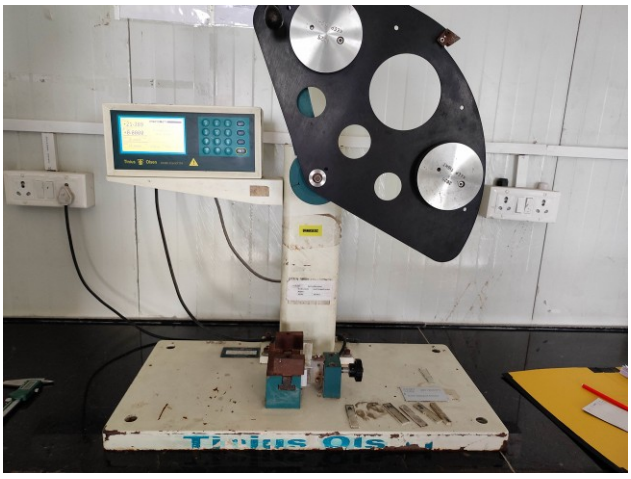

Figure 10. Sample attachment with Izod impactor testing machine

each of the specimens which is at least 4 mm away from the edge of the specimen. The average values of reading of different bioinspired configurations are recorded. The specimen setup for hardness testing is shown in Figure 11.

Figure 11. Barcol hardness tester

2.4.5 Density test

The density of all ten specimens was measured using a Saffron instrument with an accuracy of 0.1 mg. The specimen, prepared according to platform size of weighing instrument, sample had dimensions of 20 × 20 mm with a thickness of 3 mm. The digital instrument automatically measured the density based on calculation of the weight of the specimen measured both in air and water. This procedure ensured precise and reliable density measurement, and also accounted for buoyancy effects during the measurement process.

3. Results and discussion

3.1 Effect of platelet size and platelet spacing in tensile strength

Figure 12 illustrate the tensile strength of the F12 biomimetic fiber-reinforced composites was evaluated for two different configurations: varying nacre-like platelet sizes from 10 mm to 30 mm, and varying inter-platelet spacing from 2 mm to 6 mm. These results indicate that the tensile strength is influenced by variations in platelet size and inter-platelet spacing. Results reveal that values of tensile are improved by increasing the size of platelet and reverse trend observed that value degrade by increasing gap between platelet. Overall strength and modulus become lower than plain non-biomimetic composite plate due to higher tendency of material homogeneity and proper load distribution between fiber and matrix material achieved so that it promotes the distribution of stress thoroughly inside the laminate parallel between glass fiber and GP LR grade resin.

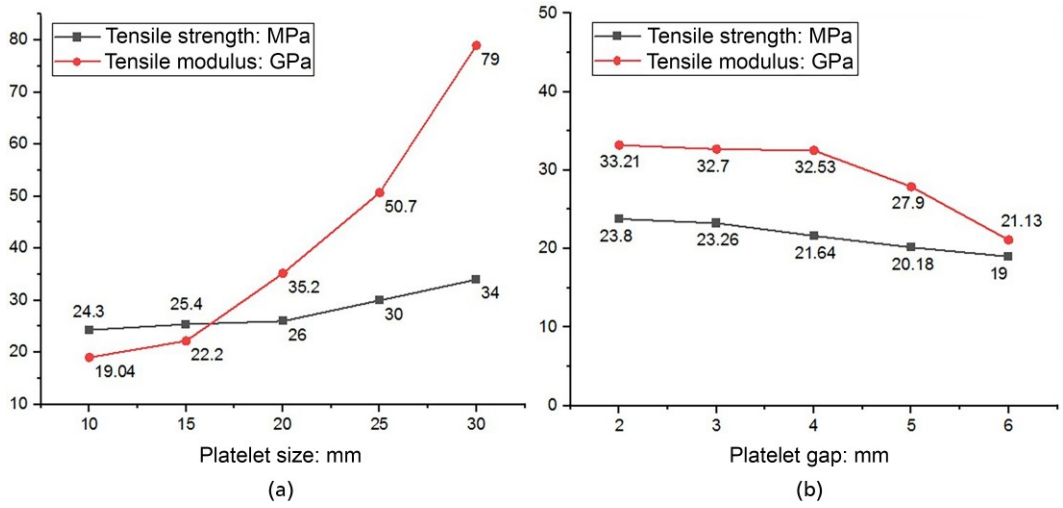

Figure 12. (Left) Platelet size (10–30 mm plotted against tensile property chart); and (right) platelet gap plotted against tensile property chart values are compared with plain laminate

Higher value of tensile strength 78 MPa and tensile modulus 87 GPa obtained at plain non-biomimetic laminate material which is greater than rest of all other combination biomimic combination laminate with same size and weight. This happened due to proper and uniform coating of fiber material with resin which allow maximum stress transfer in non-biomimetic plain laminate material. A decrease in tensile strength in bio-mimetic materials is attributed to increased discontinuity and heterogeneity between the reinforcement platelets and the resin matrix. Consequently, under axial tensile loading, the load transfer between the fibers and the matrix is inefficient, leading to a reduction in the overall tensile strength of the laminate. As per graph higher value of tensile strength is obtained for laminate having fixed gap 1 mm and higher platelet size 30 mm as compared with same size with 6 mm gap. Lowest value of tensile strength is obtained for laminate having maximum gap (interplatelet placing). Incremental trend of tensile strength is observed for laminate having fixed gap with increasing size of biomimic platelet from 10 to 30 mm. Maximum value is achieved at 34.1 MPa for laminate having platelet size 30 mm. The tensile strength decreased as the inter-platelet gap increased from 2 mm to 6 mm, with the lowest value of 19 MPa observed at the maximum gap of 6 mm. The above results represent the influence of platelet size and spacing in tensile strength of material. The results indicate that increasing the platelet size (with uniform orientation) promotes a more uniform and parallel distribution of tensile stress. In contrast, increasing the inter-platelet gap leads to localized stress concentrations, which facilitate rapid crack initiation and propagation within the laminate. Larger gaps reduce fracture strength, lower crack resistance, and allow cracks to propagate both in-plane and radially.

The above results show the effect of both the platelet size and platelet spacing on tensile properties of the biomimic composite laminate. Both parameters studied and platelet spacing have a greater impact on the composite laminate due to drastic reduction of tensile strength from highest value of 78–19 MPa lowest one in maximum platelet gap. Most concerning parameter of biomimic design is interplatelet size that directly reduces overall tensile strength of laminate under application of tensile load. While designing industrial components higher value of platelet size 30 mm and minimum gap are preferable for fabrication of laminate for satisfying maximum safety requirement.

Figures 13 and 14 demonstrate that all bioinspired composite materials with various configuration indicate a brittle nature of stress–strain profile which contains minute strain value before rapture point. Moreover, the stress–strain graph represents the bioinspired composites which exhibits the higher deformation under minimal stress condition as compared to plain laminate material. This behavior obtained through gap between the platelet promotes the significant deformation as compared to plain laminate material. Consequently, an increase in platelet sizes leads to minimized deformation and uniformly distribute the applied stress over large platelet area which enhanced tensile response clearly indicated in graph of 30 mm platelet size stress–strain behavior. Increasing the gap between platelets results in higher deformation and strain at lower stress levels due to uneven stress distribution between the fiber platelets and the matrix. This leads to a reduction in the tensile strength of the bio-inspired material compared to plain monolithic material. Higher gap between platelet leads to increasing tendency of stress polarization which promotes the crack propagation in gap between platelet and matrix material.

The composite exhibited a maximum tensile strength of 34.1 MPa when a platelet size of 30 mm and an interplatelet spacing of 1 mm were used. In contrast, increasing the spacing to 6 mm caused a

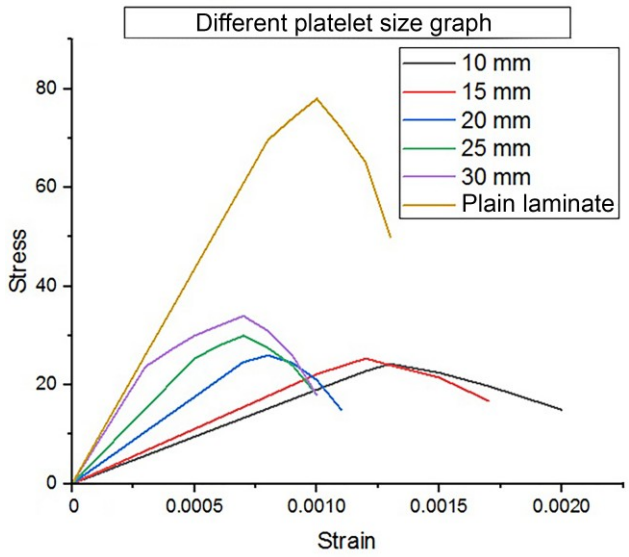

Figure 13. Stress plotted against strain plot for platelet size varies from 10 to 30 mm and compared with plain laminate graph

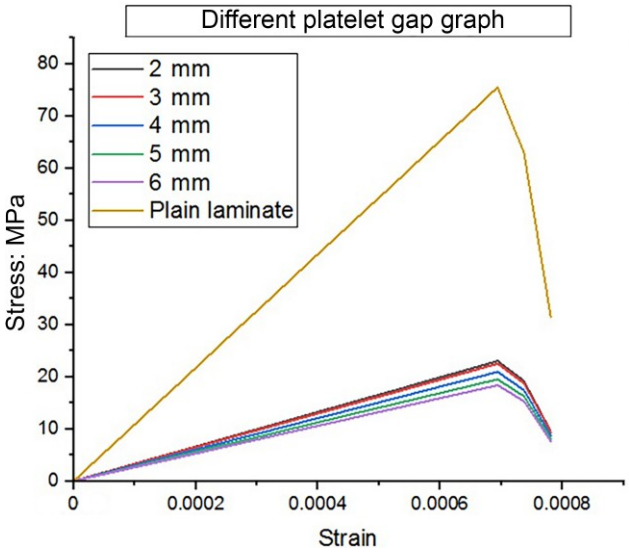

Figure 14. Stress plotted against strain plot for platelet gap varies from 2 to 6 mm and compared with plain laminate graph

significant reduction in tensile strength to 19 MPa, highlighting the adverse effect of larger gaps on load transfer efficiency and crack propagation resistance. Similarly, the optimal configuration of 30 mm platelet size and 1 mm spacing achieved a flexural strength of 127 MPa, representing a 46% improvement compared to non-bioinspired monolithic laminate materials. This improvement can be attributed to the enhanced crack resistance provided by the interlocked fiber–matrix interface. However, larger interplatelet spacings significantly reduced flexural rigidity, with the lowest flexural strength recorded at 6 mm spacing.

3.2 Flexural strength

The line chart in Figure 15 reveals the value of the flexural test results for platelet size 10–30 mm and interplatelet spacing (gap) 2–6 mm shown in Figure 16. It can be observed from the result that there is a significant improvement of flexural strength from platelet size 30 mm laminate while the lowest value of flexural strength from interplatelet spacing is maximum at 6 mm gap. Values of flexural strength and flexural modulus declined by

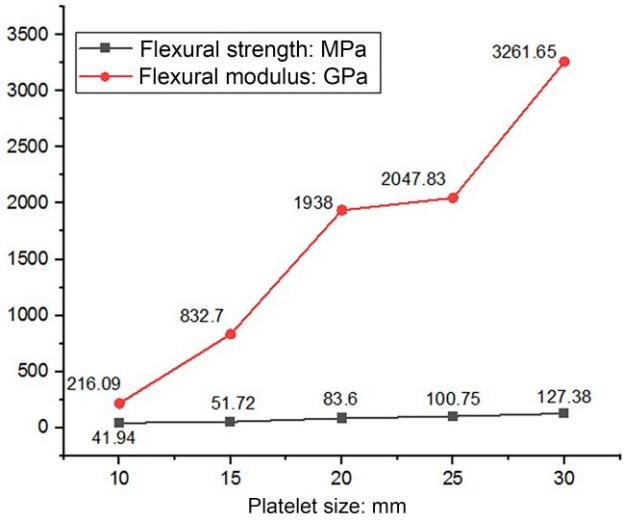

Figure 15. Flexural strength and flexural modulus of platelet size 10–30 mm

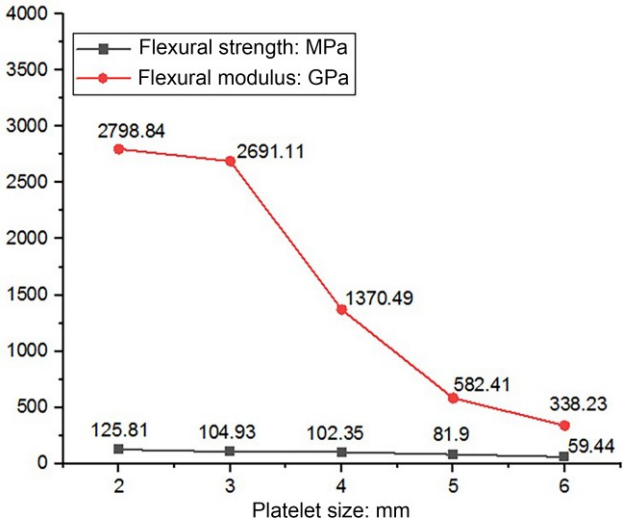

Figure 16. Flexural strength and flexural modulus of platelet gap 2–6 mm

increased the interplatelet spacing from 2 to 6 mm. The results reveal the influence of reinforcement platelet size and interplatelet spacing perform key role in flexural strength and modulus of bio-inspired composite material.

The flexural strength of laminate composite material depends on laminate structural rigidity and post yield behavior under application of three-point bending load. Flexural rigidity is reduced through development of crack or pre-existing crack and its propagation leads to the failure of laminate in brittle nature and the flexural behavior. Non-destructive testing was carried out through visual inspection procedure to assess presence of defects on surface and failure severity after conducting the flexural test. Crazing pattern on top surface on laminate is observed which indicates the deformation due to compression of laminate top layered subject to bending. Cracks in the bottom layer occurred due to the presence of microvoids formed during the manufacturing process. The development of microcracks and micro-gaps at the fiber–matrix interfaces generates high tensile stress in the bottom regions of the composite, leading to the formation of visible cracks. However, size and shape of reinforcement fiber platelet and minimum gap distribute the compressive and tensile uniformly through fiber–matrix interface and withstand maximum bending load, i.e. optimum combination of platelet size 30 mm and gap 1 mm gives maximum value of bending strength 127 MPa and modulus 3261 GPa which is greater than plain non-biomimic laminate by 46% and 35%, respectively. The nacre-like hierarchical structure interlocks the fiber–matrix interface, reducing crack propagation within the interface. This phenomenon is responsible for the higher bending strength and modulus observed in bio-inspired laminates ,in comparison with plain non-bioinspired monolithic laminates. In case of plain laminate, the interlocking mechanics is absent and crack propagation easily and rapidly happed within fiber and matrix interface that magnifying the brittle failure of laminate with application of small bending load. While decline of bending strength observed from 2 to 6 mm platelet gap and lowest value 81 MPa achieve at 6 mm inter platelet spacing in spite of maximum platelet size 30 mm happed due to increasing interface between platelet and matrix material promotes the bending load localization leads the stress concentration in matrix material lowering value of bending strength in laminate. Higher platelet size and lower gap promotes the easy stress distribution throughout the laminate promotes highest value of bending strength.

The flexural stress vs strain graph of the bioinspired epoxy-glass fiber composite is shown in Figures 17 and 18, which clearly indicates the influence homogeneous and continuous distribution of platelets within bioinspired composite material. The laminate with a platelet size of 30 mm contains the highest slope over the non-bioinspired plain laminate and other bioinspired configurations. This can be obtained by the uniform distribution of bending loads over a larger area having higher platelet size which effectively improving resistance to deformation. The larger platelet size facilitates improved load transfer capabilities and minimizing localized

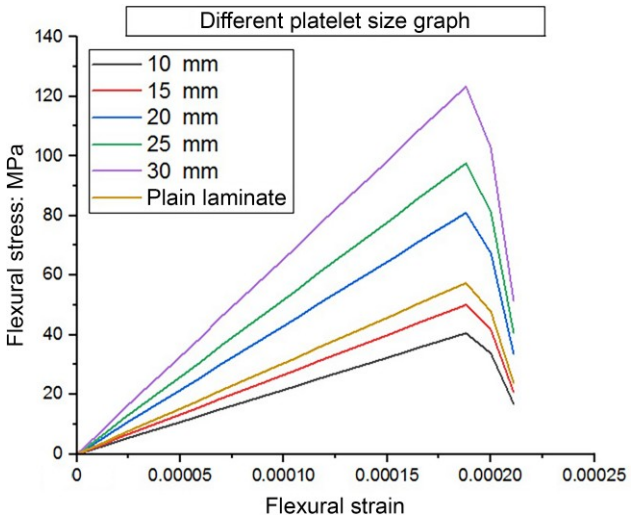

Figure 17. Flexural stress plotted against flexural strain graph for platelet size varies from 10 to 30 mm and compared with plain laminate graph

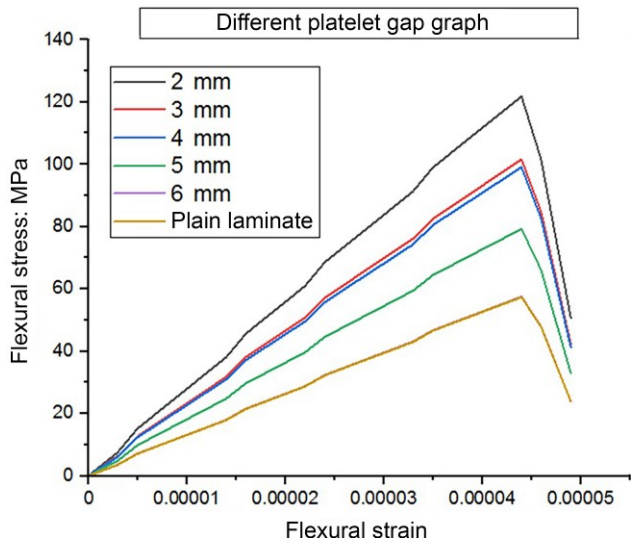

Figure 18. Flexural stress plotted against flexural strain graph for platelet gap varies from 2 to 6 mm and compared with plain laminate graph

stress concentrations so that it enhancing the overall flexural strength. Moreover, reducing the gap between platelets also promotes the bending strength by uniform stress distribution; however, the flexural strength remains comparatively lower at with larger platelet size. Consequently, an optimal platelet size of 30 mm is observed as the most effective configuration for achieving maximum flexural strength value due to as its superior bending loads resistance capacity with minimal deformation. Higher platelet size leads the increasing the interlocking tendency

between fiber and matrix interface leads to increasing flexural load bearing capacity.

3.3 Impact strength

Figure 19 provides the Izod impact strength for bioinspired nacre like platelet e-glass fiber reinforcement polyester resin composite material and it reflects variation of the impact strength gradually improved with the increase in platelet size and gap up to 25 mm platelet size and gap 5 mm but after that values are decreasing. These results clearly depict the influence of platelet size and gap on impact strength of nacre like bioinspired composite material. Performance of bioinspired laminate under impact load gives an important trend that the improvement of impact strength happened by incorporating optimum platelet size and gap that add structural heterogeneity and lower crystallinity which dissipate and absorb the impact energy. The brick-mortar and nacre like platelet structure minimize the crack propagation which reduced the sudden impact failure of laminate. Lowest value of impact strength observed at platelet size 10 mm and gap 2 mm which indicates the energy distribution between fiber and matrix material not attained properly with low platelet size of reinforcement that leads to formation of micro-cracks during impact loading. While increasing platelet size up to 25 mm gives highest possible values of impact strength after that further increasing platelet lead to decreasing the impact strength that promotes structural homogeneity at higher value of platelet size after 25 mm that promotes the crack propagation easy and rapid within laminate and reducing impact strength. However, impact strength of plain laminate (1.98 J/mm) becomes lower than bioinspired nacre like platelet composite material (2.345 J/mm) which shows the improvement of impact strength by 84.4% than non-biomimic material due nacre like structure having greater tendency for absorbing and dissipating impact energy and also reduced crack propagation within laminate. Increasing inter platelet spacing leads slight increasing in impact strength up to 5 mm gap, after further increasing the gap minimize the value of impact strength which is lower than plain laminate material, this happened due to increasing the gap between platelet promotes the micro voids and reduced the stiff material interface with matrix material cause the weakening the material impact strength through impact load concentration and proper dissipation not achieved.

3.4 Hardness test

The results obtained through Barcol hardness tester as per the ASTM D 2583[59–63] standard are mentioned in Figure 20. The results show the effect of bioinspired platelet size and interplatelet on hardness of nacre like composite material. Values of hardness increase with increasing platelet size maximum at 30 mm platelet size with 49 BHN values and reverse trend observed from increasing interplatelet gap 2–6 mm, low value 40 BHN observed at maximum platelet gap 6 mm. plain laminate possess the highest value 56 BHN for both nacre like (i.e. platelet size variation and platelet gap variation) composite material configuration. Maximum hardness value obtained in plain laminate compared with nacre like composite material due to continues and dense distribution glass fiber content increased the overall hardness value unlike in biomimic laminate having platelet orientation and gap cause the discontinuity and lowering fiber density on outer surface leads the declining hardens value of laminate.

Higher value of platelet size in bioinspired composite material exhibits large surface area of glass fiber content on outer surface morphology which leads to higher value of wear resistance properties offered by this composition which is comparatively higher than other platelet size. Higher platelet size also increased glass content on surface which promotes the higher wear resistance than any other composite. Reverse trend observed while increasing gap between platelet, that is, 2–6 mm, leads to reduce the glass content on outer surface reduce the wear resistance capacity. However, the plain monolithic laminate having maximum possible glass content possess highest value of hardness and wear resistance.

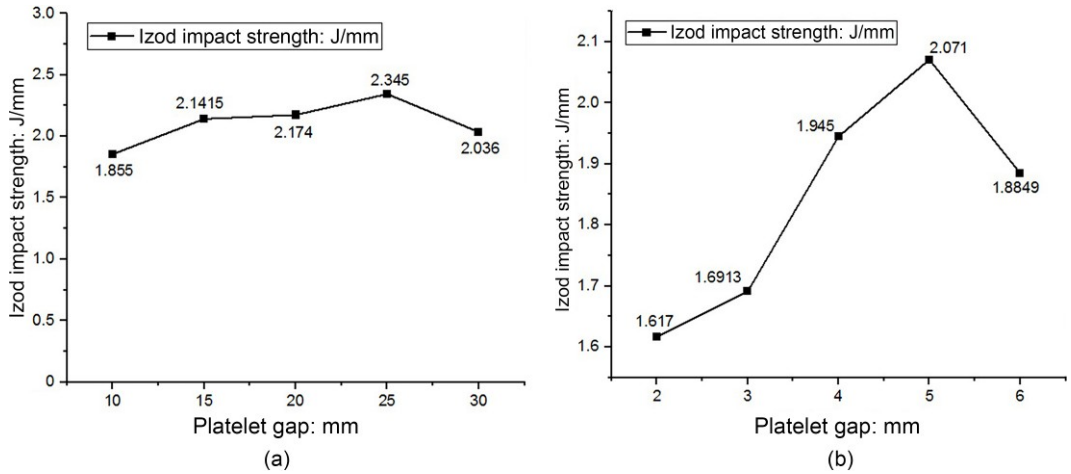

Figure 19. (Left) Izod impact strength of platelet size 10–30 mm; (right) platelet gap 2–6 mm

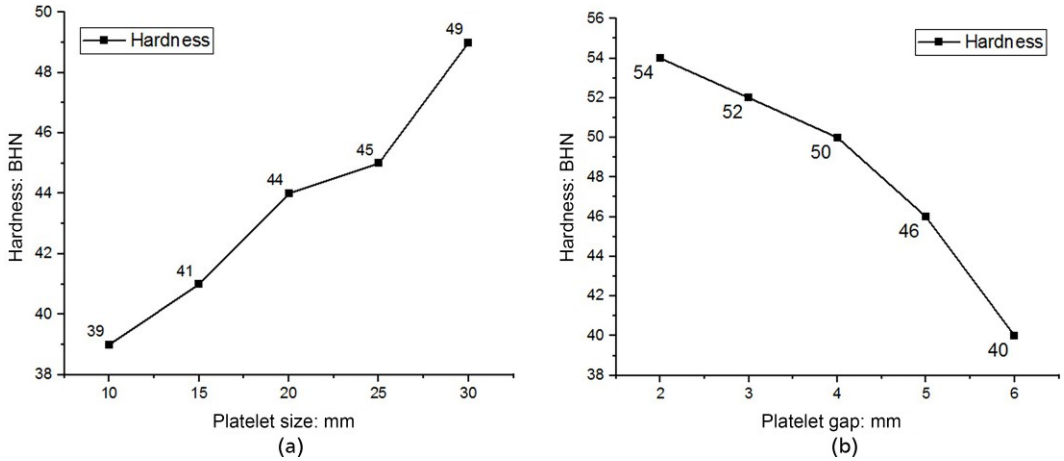

Figure 20. (Left) Barcol hardness value of platelet size varied 10–30 mm; (right) platelet gap 2–6 mm

3.5 Density test

Figure 21 shows the physical properties (i.e. density) variation with platelet size and interplatelet gap and these two configurations directly compare with plain laminate (non-biomimic composite material). The results indicate the effect of platelet size and platelet gap on density of composite material having maximum values obtained by plain laminate material with value 3.125 g/cm^3. While in bioinspired material values of density increased with increasing size of platelets from 10 to 30 mm with density values increasing from 1.0219 to 2.6071 g/cm^3. The reduction in overall laminate density is influenced by platelet size and inter-platelet spacing. An increasing trend in density is observed with larger platelet sizes, as they result in a higher fiber content within the laminate, increasing both area density and volumetric density. Conversely, increasing the inter-platelet gap reduces the area density of glass fiber platelets. Larger gaps also cause fiber–matrix interference, leading to the formation of micro-voids within the laminate, which further decreases the overall density. In the plain laminate configuration, the fiber density is maximized, resulting in the highest density value of 3.125 g/cm^3 among all variants of the bio-inspired laminates.

The density value increases with increasing platelet sizes (10–30 mm), represent the influence of glass fiber content, which is responsible for a higher overall density value due to its greater density compared to the epoxy resin matrix material. A larger platelet size (i.e. 30 mm) results in an increased concentration of glass fiber population within the matrix and also dense packing between matrix and fiber which leads to enhancing the composite's density. Conversely, an opposite behavior is observed when the gap between platelets increases from 2 to 6 mm, as this phenomenon promotes the higher gap between platelet and matrix have a higher tendency for void formation due to inadequate matrix infiltration between the platelets leads to lowering density value like lowest

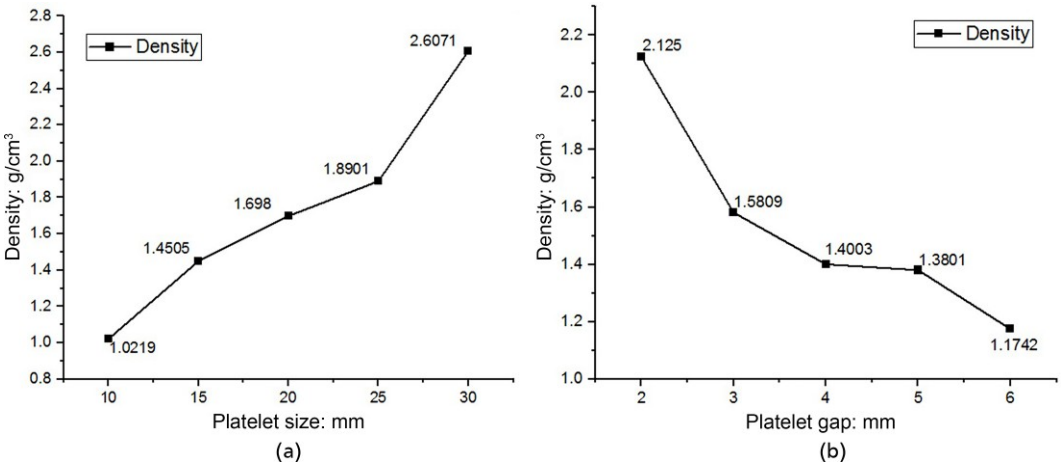

Figure 21. (Left) Density value for platelet size 10–30 mm; (right) platelet gap 2–6 mm

value observed at gap 6 mm. While the maximum value density observed at plain laminate configuration having maximum possible glass content within fiber matrix interface.

3.6 SEM result and interpretation

SEM inspections conducted on the bioinspired laminates and the conventional laminate revealed the microstructural features associated with their respective failure mechanisms during tensile testing.[64–70] Figure 22 presents the SEM image of the cross-section of the conventional laminate and bioinspired laminate. Plain laminate exhibits severe damage at the fiber–matrix interface, including complete delamination of the fiber and matrix system. This behavior is primarily attributed to the absence of an interlocking mechanism between the fiber platelets and the epoxy matrix structure. The homogeneous and uniform arrangement of E-glass fibers within the matrix material facilitates crack propagation along the fiber–matrix interfaces, ultimately resulting in the weakening of the composite structure.

In contrast, SEM analysis of the bioinspired laminates, characterized by a heterogeneous distribution of fiber platelets and matrix interfaces, demonstrated improved load transfer and enhanced crack-arresting capabilities. This microstructure of the bioinspired laminates, which exhibits higher stiffness, resulted in minimal delamination between the fiber and matrix, and the bonding between the fiber platelets and the matrix material remained largely unaffected under tensile loading conditions. Figures depict the microscopic observations of two bioinspired laminates containing platelet sizes of 30 mm, which showed the highest tensile strength, and laminates with a maximum platelet gap of 8 mm, which exhibited the lowest tensile strength, respectively. Both bioinspired laminates demonstrated significantly less damage to the fiber–matrix bonding compared to the conventional laminate material.

3.7 X-ray diffraction result

Figure 23 shows the X-ray diffraction[71–74] patterns of the plain E-glass epoxy laminate and the two bioinspired epoxy glass fiber composites (i.e. 30 mm platelet size and 6 mm gap) indicates the characteristic features of partially amorphous nature of polymeric matrix reinforced with crystalline silica phases (glass phase). All three samples exhibited a various diffraction peak at approximately value $2\theta \approx 7.22°–7.23°$, with a high intensity close to 800 000 counts and corresponding to reflections obtained from the glass fiber reinforcement. A secondary reflection shows the consistently near value $2\theta \approx 28.5°–28.8°$, represent the crystalline contributions of silicate phases. Compared to the plain laminate, the bioinspired composites displayed a marginally broader background and slightly higher baseline intensity value in the low-angle region, suggesting a minor increase in amorphous content and the presence organic material. Among the three graph, the first graph (plain laminate) showed the sharpest diffraction peaks and the lowest background intensity which denotes the higher structural uniformity, homogenous distribution of fiber and matrix material and lower microstructural disorder. The second and third bioinspired composites represent comparable characteristics, with the third sample having maximum showing a subtly higher degree of diffuse scattering, potentially reflecting more extensive

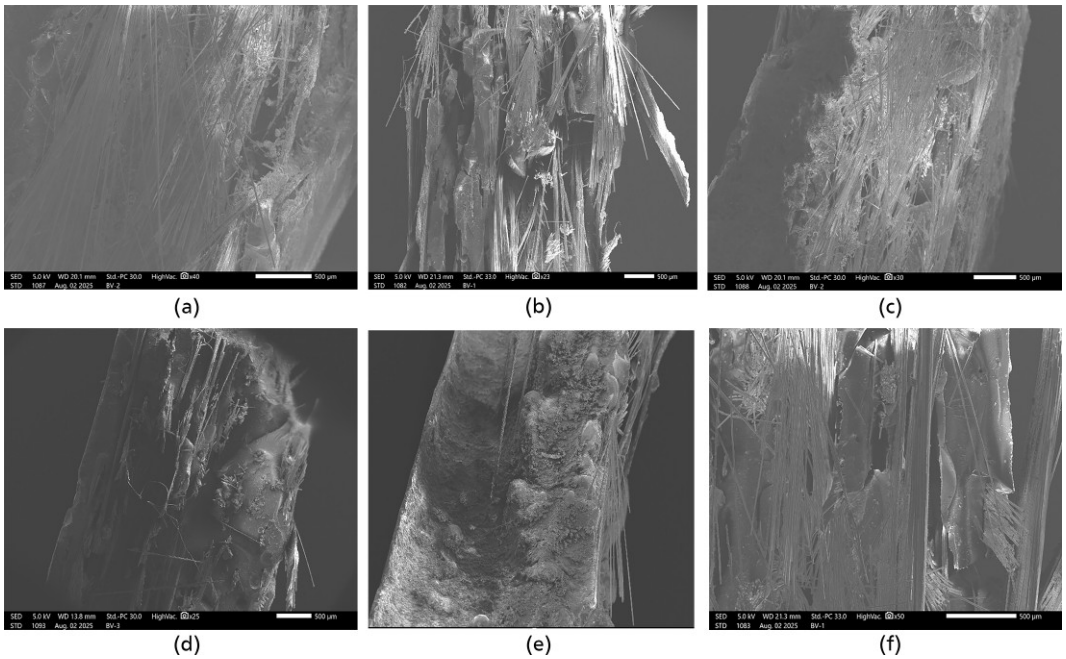

Figure 22. SEM image of conventional laminate and bioinspired laminate

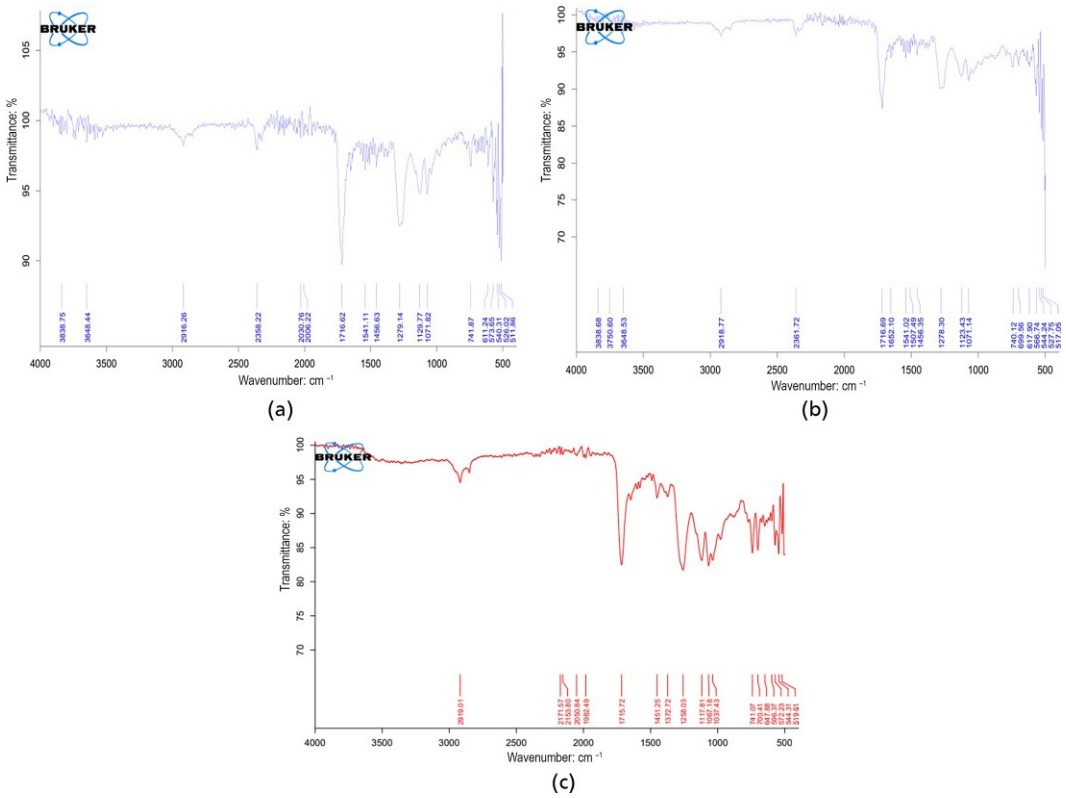

Figure 23. XRD result of conventional plain laminate and bioinspired laminate

dispersion of bioinspired reinforcements within the matrix. Overall, while all samples demonstrated effective incorporation of glass fiber phases, the plain laminate exhibited the most well-defined crystalline reflections and the least amorphous scattering.

3.8 FTIR result

Fourier transform infrared spectroscopy (FTIR) analysis was performed on both bioinspired and plain laminae composite samples to examine their chemical structure and functional group characteristics. Figure 24 clearly depict the result of plain E-glass epoxy laminate (Sample 1) characteristic absorption bands achieved near 2920 cm^{-1} corresponding to C–H stretching vibrations, and strong bands between 1250 and 1030 cm^{-1} attributed to C–O–C stretching of the epoxy matrix system. In Sample 2 (bioinspired composite with platelet size 30 mm) having peaks appeared with increased transmittance and sharper definition, particularly the band near 1720 cm^{-1} indicating C=O stretching of ester or carbonyl groups which indicates the higher degree of cross-linking through better resin curing process. Furthermore, Specimen 2 having higher platelet size shows distinct peaks in the region (around 700–500 cm^{-1}), possibly reflecting interactions between the bioinspired platelet orientation and epoxy matrix. Sample 3 (bioinspired composite with platelet gap 6 mm) similarly showed prominent peaks near 1715 and 1240 cm^{-1}, but the overall transmittance levels were slightly lower than Sample 2 indicating the moderate level matrix–filler interaction. Compared to the plain conventional laminate, both bioinspired composites presented more defined and intense absorption capability, indicating enhanced chemical interactions and potentially improved network structure. Among them, Sample 2 exhibited the most prominent carbonyl and ether functional group bands, reflecting a higher cross-link density and better phase integration.

Table 1 provides a brief overview of the mechanical properties that includes the value of tensile strength, flexural strength, Izod impact resistance, density, and hardness which is obtained through various relevant testing procedures. These mentioned properties are directly compared with bioinspired composite materials having different configurations like variations in platelet size and gap, as detailed in the subsequent section. This comparative analysis aims to assess the significant of structural modifications on the overall mechanical performance of the bioinspired advanced composite materials.

4. Conclusions

This study systematically outlines the effect of platelet size and interplatelet spacing on the mechanical properties of bioinspired nacre-like composite materials. The results are reflected that optimizing these parameters significantly improves tensile strength, flexural strength, impact resistance, hardness, and density.

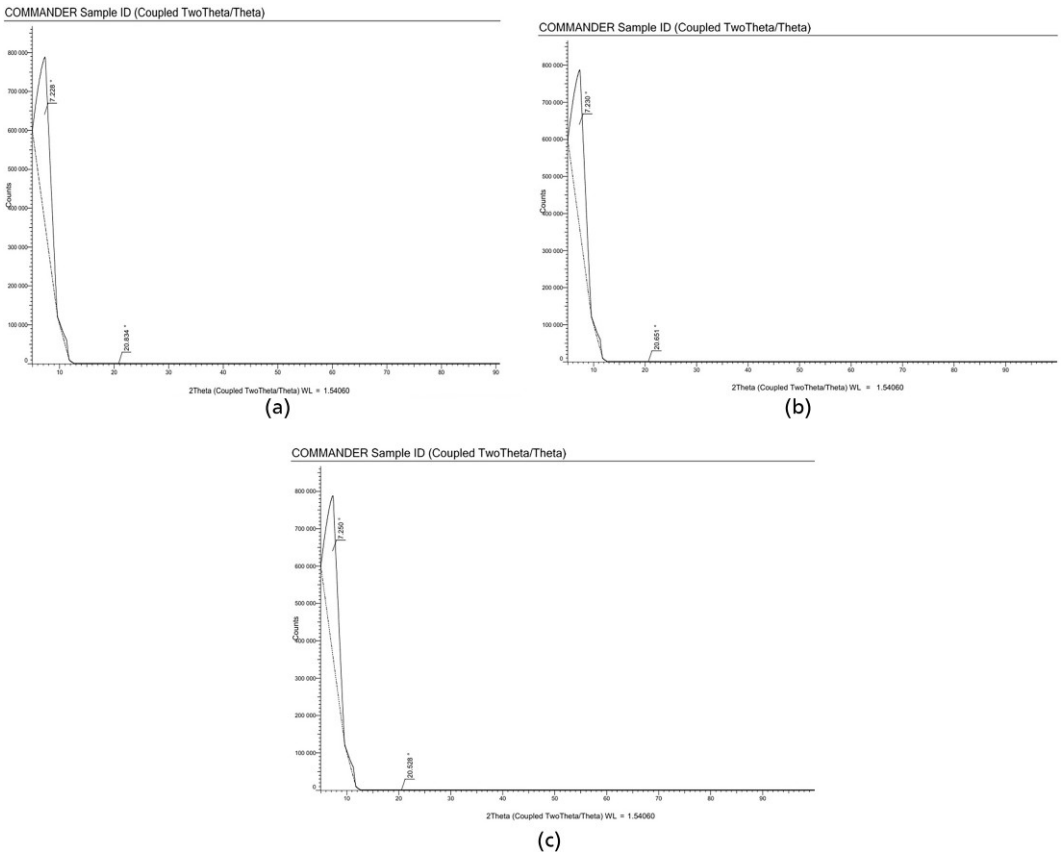

Figure 24. FTIR result of plain laminate and bioinspired structure

Table 1. Mechanical properties overview for plain laminate and bio-mimic laminate

	Plain laminate (non-biomimic composite)		Biomimetic composite									
			Fixed platelet size: mm					Platelet gap: mm				
Sr. no.	Mechanical properties	Value	10	15	20	25	30	2	3	4	5	6
1	Tensile strength: MPa	78	24.3	25.4	26	30	34	23.8	23.26	21.64	20.18	19
2	Tensile modulus: GPa	87	19	22.2	35.2	50.7	79	33.2	32.7	32.5	27.9	21.1
3	Flexural strength: MPa	59.29	41.94	51.72	83.6	100.75	127.38	125	104	102	81	59
4	Flexural modulus: GPa	1168	216	832	1938	2047	3261	2798	2691	1370	582	338
5	Izod impact strength: J/mm	1.98	1.8	2.1	2.17	2.3	2	1.6	1.7	1.9	2	1.8
6	Hardness: BHN	56	39	41	44	45	49	54	52	50	46	40
7	Density: g/cm^3	3.12	1.1	1.4	1.6	1.8	2.6	2.1	1.5	1.4	1.3	1.17

Notably, a platelet size of 30 mm having an interplatelet spacing of 1 mm resulted in the highest tensile strength of 34.1 MPa and flexural strength of 127 MPa which indicates a 46% improvement over conventional non-bioinspired plain laminates. The improved mechanical properties are subject to enhancement of crack resistance and efficient stress distribution within the fiber–matrix interface. However, increasing interplatelet spacing to 6 mm reduced load transfer and distribution capacity which leads to a gradient reduction in both tensile and flexural strengths. Experimental results revealed that the minimum tensile strength was observed for a platelet size of 10 mm, with a value of 24.3 MPa. In contrast, the maximum tensile strength reached 34 MPa for the specimen with a platelet size of 30 mm, indicating enhanced load transfer capability due to the larger platelet dimensions. Furthermore, the effect of platelet gap was found to be significant; an increase in the gap between platelets resulted in a decline in tensile performance. Specifically, specimens with a 2 mm gap exhibited a tensile strength of 23.8 MPa, whereas those with a 6 mm gap showed a

reduced value of 19 MPa. This reduction suggests a weakening of the stress distribution and interfacial bonding between the platelet, fiber, and matrix phases at wider gaps. These findings confirm that both platelet size and spacing are critical parameters influencing the mechanical behavior of bioinspired composite laminates.

The hardness and density measurements show a direct relation between platelet size and material compactness. Larger platelet sizes contributed to higher density and hardness due to increased fiber content on surface morphology. However, bioinspired configurations contain the slightly lower values as compared to monolithic laminates, which can be attributed to the uniform fiber distribution over entire surface area. These notions provide valuable insights for tailoring high-performance bioinspired composites designed for structural applications. The optimized configurations of given parameters (i.e. platelet size and spacing) observed in this work reflect the potential of such materials for utilization in impact-resistant automotive components like crash boxes, bumper beams, and engine splash bottom covers.

FTIR analysis revealed higher peak intensities at 915 and 1250 cm^{-1} for the bioinspired laminate, indicating improved epoxy curing and ≈18%–22% stronger interfacial bonding compared to the conventional laminate. X-ray diffraction (XRD) results showed an increase in crystallinity index from 62.4% (conventional) to 71.8% (bioinspired, 30 mm platelet), along with a reduction in calculated crystallite size from 5.8 to 4.9 nm, suggesting lower residual stress. SEM analysis demonstrated a decrease in fiber–matrix delamination width from ≈14.2 µm (conventional) to ≈6.5 µm (bioinspired, 30 mm platelet), correlating with the highest tensile strength, while the 8 mm platelet variant exhibited moderate performance with ≈9.4 µm delamination.

However, the composites in this study were fabricated using the hand layup process, which may introduce variability in the results. However, automating the manufacturing process could enhance repeatability and improve the accuracy of the findings.

REFERENCES

1. Ghazlan A, Ngo T, Tan P *et al.* (2021) Inspiration from nature's body armours a review of biological and bioinspired composites. In *Composites Part B: Engineering*, p. 205.
2. Madhav D, Buffel B, Moldenaers P *et al.* (2023) A review of nacre-inspired materials: chemistry, strengthening-deformation mechanism, synthesis, and applications. *Progress in Materials Science* **139**: 101168, 10.1016/j.pmatsci.2023.101168.
3. Chen Q and Pugno NM (2013) Bio-mimetic mechanisms of natural hierarchical materials: a review. *Journal of the Mechanical Behavior of Biomedical Materials* **19**: 3–33, 10.1016/j.jmbbm.2012.10.012.
4. Ha NS and Lu G (2020) A review of recent research on bio-inspired structures and materials for energy absorption applications. *Composites Part B: Engineering* **181**: 107496, 10.1016/j.compositesb.2019.107496.
5. Sharma A, Shukla NK, Belarbi M-O *et al.* (2023) Bio-inspired nacre and helicoidal composites: from structure to mechanical applications. *Thin-Walled Structures* **192**: 111146, 10.1016/j.tws.2023.111146.
6. Naleway SE, Taylor JRA, Porter MM *et al.* (2016) Structure and mechanical properties of selected protective systems in marine organisms. *Materials Science & Engineering. C, Materials for Biological Applications* **59**: 1143–1167, 10.1016/j.msec.2015.10.033.
7. Naleway SE, Porter MM, McKittrick J *et al.* (2015) Structural design elements in biological materials: application to bioinspiration. *Advanced Materials (Deerfield Beach, Fla.)* **27(37)**: 5455–5476, 10.1002/adma.201502403.
8. Meyers MA, McKittrick J and Chen P-Y (2013) Structural biological materials: critical mechanics-materials connections. *Science (New York, N.Y.)* **339(6121)**: 773–779, 10.1126/science.1220854.
9. Meyers MA, Chen P-Y, Lopez MI *et al.* (2011) Biological materials: a materials science approach. *Journal of the Mechanical Behavior of Biomedical Materials* **4(5)**: 626–657, 10.1016/j.jmbbm.2010.08.005.
10. Meyers MA, Chen P-Y, Lin AY-M *et al.* (2008) Biological materials: structure and mechanical properties. *Progress in Materials Science* **53(1)**: 1–206, 10.1016/j.pmatsci.2007.05.002.
11. Fratzl P and Weinkamer R (2007) Nature's hierarchical materials. *Progress in Materials Science* **52(8)**: 1263–1334, 10.1016/j.pmatsci.2007.06.001.
12. Sun J and Bhushan B (2012) Hierarchical structure and mechanical properties of nacre: a review. *RSC Advances* **2(20)**: 7617–7632, 10.1039/c2ra20218b.
13. Wei X, Filleter T and Espinosa HD (2015) Statistical shear lag model unraveling the size effect in hierarchical composites. *Acta Biomaterialia* **18**: 206–212, 10.1016/j.actbio.2015.01.040.
14. Gebremaryam G, Shahapurkar K, Chenrayan V *et al.* (2025) The structural and thermal integrity of novel bio-polymer composite processed from Ethiopian teff husk particles for constructional applications. *Journal of Polymer Research* **32(1)**, 10.1007/s10965-02404239-2.
15. Shahapurkar K, Ramesh S, Nik-Ghazali N-N *et al.* (2024) Tensile, compressive, and fracture behavior of Habeshian chopped banana/epoxy core sandwich woven banana composite. *Biomass Conversion and Biorefinery* **14(17)**: 21553–21564, 10.1007/s13399-024-05455-y.
16. Alghataibeh S, Wan H, Al-Fodeh R *et al.* (2022) Fabrication and mechanical properties of biomimetic nacre-like ceramic/polymer composites for chairside CAD/CAM dental restorations. *Dental Materials: Official Publication of the Academy of Dental Materials* **38(1)**: 121–132, 10.1016/j.dental.2021.10.016.
17. Wu H, Guo A, Kong D *et al.* (2024) Nacre-like carbon fiber-reinforced biomimetic ceramic composites: fabrication, microstructure, and mechanical performance. *Ceramics International* **50(14)**: 25388–25399, 10.1016/j.ceramint.2024.04.270.
18. Chen X-H, Wang F, Zhang Z *et al.* (2024) Enhanced mechanical properties of Ti3C2Tx MXene/Al composites with nacre-inspired laminated architecture. *Journal of Alloys and Compounds* **987**: 174180, 10.1016/j.jallcom.2024.174180.
19. Zhang J, Zhang X, Qian M *et al.* (2024) Nacre-like hybrid aluminum-matrix composite with simultaneously enhanced strength and toughness. *Composites Part A: Applied Science and Manufacturing* **187**: 108480, 10.1016/j.compositesa.2024.108480.
20. Nie M, Lin B, Chen Y *et al.* (2025) High temperature mechanical properties and tribological behavior of nacre-inspired Ti (C, N)/Al-Cu composites. *Tribology International* **202**: 110288, 10.1016/j.triboint.2024.110288.
21. Liu F, Lu X, Jin G *et al.* (2024) Bulk graphene-based composites with artificial nacre-like laminated structure: microstructure and mechanical properties. *Materials Today Communications* **40**: 109873, 10.1016/j.mtcomm.2024.109873.

22. He L, Si S, Xu H *et al.* (2020) Enhanced mechanical property and radiation resistance of reduced graphene oxide/tungsten composite with nacre-like architecture. *Composite Structures* **245**: 112361, 10.1016/j.compstruct.2020.112361.
23. Liu S, Yao F, Oderinde O *et al.* (2017) Zinc ions enhanced nacre-like chitosan/graphene oxide composite film with superior mechanical and shape memory properties. *Chemical Engineering Journal* **321**: 502–509, 10.1016/j.cej.2017.03.087.
24. Gurbuz SN and Dericioglu AF (2013) Effect of reinforcement surface functionalization on the mechanical properties of nacre-like bulk lamellar composites processed by a hybrid conventional method. *Materials Science & Engineering. C, Materials for Biological Applications* **33(4)**: 2011–2019, 10.1016/j.msec.2013.01.013.
25. Peng W, Ge Z, Shao Y *et al.* (2024) Mechanical behavior of nacre-inspired CFRP composites by 3D printing. *Composite Structures* **339**: 118167, 10.1016/j.compstruct.2024.118167.
26. Song S, Wu Q, Ji D *et al.* (2024) Nacre-inspired composite paper of PVA crosslinked basalt scale and nanocellulose with enhanced mechanical, electrical insulating and ultraviolet-resistant aging performance. *International Journal of Biological Macromolecules* **257(Pt 1)**: 128602, 10.1016/j.ijbiomac.2023.128602.
27. Ji D, Zhang M, Sun H *et al.* (2025) Nacre-inspired composite papers with enhanced mechanical and electrical insulating properties: assembly of aramid papers with aramid nanofibers and basalt nanosheets. *Journal of Materials Science & Technology* **215**: 283–295, 10.1016/j.jmst.2024.07.044.
28. Gao K, Tan G, Liu Y *et al.* (2024) Compression fatigue properties of bioinspired nacre-like composites compared with natural nacre: effects of architectures and orientations. *International Journal of Fatigue* **179**: 108062, 10.1016/j.ijfatigue.2023.108062.
29. Ingrole A, Aguirre TG, Fuller L *et al.* (2021) Bioinspired energy absorbing material designs using additive manufacturing. *Journal of the Mechanical Behavior of Biomedical Materials* **119**: 104518, 10.1016/j.jmbbm.2021.104518.
30. Evans AG, Suo Z, Wang RZ *et al.* (2001) Model for the robust mechanical behavior of nacre. *Journal of Materials Research* **16(9)**: 2475–2484, 10.1557/JMR.2001.0339.
31. Lin AY-M and Meyers MA (2009) Interfacial shear strength in abalone nacre. *Journal of the Mechanical Behavior of Biomedical Materials* **2(6)**: 607–612, 10.1016/j.jmbbm.2009.04.003.
32. Ginzburg D, Pinto F, Iervolino O *et al.* (2017) Damage tolerance of bio-inspired helicoidal composites under low velocity impact. *Composite Structures* **161**: 187–203, 10.1016/j.compstruct.2016.10.097.
33. Patel P and Adalja D (2024) Determination of optimum parameters for the design of composite shaft. *Suranaree Journal of Science and Technology* **31(2)**: 010297, 10.55766/sujst-2024-02-e02719.
34. Tabet Zatla A, Hammoudi A, Fellah M *et al.* (2024) In vitro study of the antihemolytic and antioxidant potential of two essential oils from Salvia officinalis L. and Curcuma longa L. against glucantime® toxicity. *Journal of Engineering Research*, 10.1016/j.jer.2024.12.007.
35. Boumous S, Boumous Z, Latreche S *et al.* (2025) Investigation of the space charge dynamic in the nanocomposite $BATIO_3$-doped XLPE. *Journal of Electronic Materials* **54(1)**: 859–877, 10.1007/s11664-024-11610-y.
36. Rim I, Hezil N, Fellah M *et al.* (2024) Enhancing kaolin performance through organic molecule modification and assessing its efficiency for lead and copper adsorption. *Environmental Technology & Innovation* **36**: 103904, 10.1016/j.eti.2024.103904.
37. Zerouali M, Bouras D, Daïra R *et al.* (2025) Effect of aluminum-modified copper oxide thin films on structural, morphological, optical, and electrical properties for photocatalysis application. *Ceramics International* **51(1)**: 473–490, 10.1016/j.ceramint.2024.11.026.
38. Bouras D, Fellah M, Barille R *et al.* (2025) Comparative study of zirconium-zinc oxide thin films on ceramic and glass substrates: Structural, optical, and photocatalytic properties. *Inorganic Chemistry Communications* **171**: 113561, 10.1016/j.inoche.2024.113561.
39. Fellah M, Hezil N, Bouras D *et al.* (2024) Microstructural and photocatalytic properties of nanostructured near-β Ti-Nb-Zr alloy for total hip prosthesis use. *Kuwait Journal of Science* **51(4)**: 100276, 10.1016/j.kjs.2024.100276.
40. Fellah M, Samad MA, Labaiz M, Assala O and Iost A (2015) Sliding friction and wear performance of the nano-bioceramic α-Al_2O_3 prepared by high energy milling. *Tribology International* **91**: 151–159, 10.1016/j.triboint.2015.07.006.
41. Toualbia K, Fellah M, Hezil N, Milles H and Djafia Z (2024) Effect of milling time on structural, mechanical and tribological properties of nanostructured HIPed near type Ti-15Mo alloys. *Tribology International* **197**: 109731, 10.1016/j.triboint.2024.109731.
42. Bouras D, Fellah M, Habeeb MA *et al.* (2024) Structural and antibacterial activity of developed nano-bioceramic DD3/ZrO2/ZnO/CuO powders. *Journal of the Korean Ceramic Society* **61(5)**: 837–853, 10.1007/s43207-024-00398-6.
43. Fellah M, Hezil N, Bouras D *et al.* (2024) Investigating the effect of Zr content on electrochemical and tribological properties of newly developed near β-type Ti-alloys (Ti–25Nb-xZr) for biomedical applications. *Journal of Science: Advanced Materials and Devices* **9(2)**: 100695, 10.1016/j.jsamd.2024.100695.
44. Chandra TO, Sentanu DA, Gornes W *et al.* (2022) Tensile properties of epoxy resin filled with activated carbon derived from coconut shell. *Materials Today: Proceedings* **66**: 2967–2971, 10.1016/j.matpr.2022.06.568.
45. Rodrigues S, Miri S, Cole RG *et al.* (2023) Towards optimization of polymer filament tensile test for material extrusion additive manufacturing process. *Journal of Materials Research and Technology* **24**: 8458–8472, 10.1016/j.jmrt.2023.05.088.
46. Woods MC, Brooks CK and Pearce JM (2024) Open-source cold and hot scientific sheet press for investigating polymer-based material properties. *HardwareX* **19**: e00566, 10.1016/j.ohx.2024.e00566.
47. Raffik R, Sivaguru J, Sabitha B *et al.* (2024) Experimental investigation on Stereolithography process parameter optimization and its influence on smooth surface finish for ABS Accura-60 material. *Materials Today: Proceedings*.
48. Laureto JJ and Pearce JM (2018) Anisotropic mechanical property variance between ASTM D638-14 type i and type iv fused filament fabricated specimens. *Polymer Testing* **68**: 294–301, 10.1016/j.polymertesting.2018.04.029.
49. Rahman F, Dey DC, Tamim TM *et al.* (2024) Mechanical characterizations of waste face masks reinforced polyester composites: recycling wastes into resources. *Heliyon* **10(19)**: e38330, 10.1016/j.heliyon.2024.e38330.
50. Pradeep V, Kumar P and Reddy IR (2024) Investigation on mechanical properties and wear behavior of basalt fiber and SiO2 nanofillers reinforced composites. *Results in Engineering* **23**: 102722, 10.1016/j.rineng.2024.102722.
51. Bajracharya RM, Bajwa DS and Bajwa SG (2017) Mechanical properties of polylactic acid composites reinforced with cotton gin waste and flax fibers. *Procedia Engineering* **200**: 370–376, 10.1016/j.proeng.2017.07.052.
52. Amir N, Abidin KAZ and Shiri FBM (2017) Effects of fibre configuration on mechanical properties of banana fibre/PP/MAPP natural fibre reinforced polymer composite. *Procedia Engineering* **184**: 573–580, 10.1016/j.proeng.2017.04.140.
53. Takoumbe C, Tiaya EM, Ndapeu D *et al.* (2023) Selected physical and mechanical properties of the oil palm pseudo-trunk: case of the Tenera variety from Cameroon. *Results in Materials* **17**: 100354, 10.1016/j.rinma.2022.100354.

54. Costa UO, Nascimento LFC, Garcia JM *et al.* (2020) Evaluation of Izod impact and bend properties of epoxy composites reinforced with mallow fibers. *Journal of Materials Research and Technology* **9(1)**: 373–382, 10.1016/j.jmrt.2019.10.066.
55. Kim C-U, Kim S-J, Park J-C *et al.* (2015) Fabrication and evaluation of mechanical properties of CF/GNP composites. *Procedia Manufacturing* **2**: 368–373, 10.1016/j.promfg.2015.07.065.
56. Murthy VCAD and Santhanakrishnanan S (2020) Isogrid lattice structure for armouring applications. *Procedia Manufacturing* **48**: e1–e11, 10.1016/j.promfg.2020.05.099.
57. Venkatesh R, Ballal S, Krishnan AM *et al.* (2023) Effect of fiber layer formation on mechanical and wear properties of natural fiber filled epoxy hybrid composites. *Heliyon* **9(5)**: e15934, 10.1016/j.heliyon.2023.e15934.
58. Agrawal AP, Kumar V, Kumar J *et al.* (2023) An investigation of combined effect of infill pattern, density, and layer thickness on mechanical properties of 3D printed ABS by fused filament fabrication. *Heliyon* **9(6)**: e16531, 10.1016/j.heliyon.2023.e16531.
59. Hofmann M, Machado M, Shahid A *et al.* (2023) Pultruded carbon fibre reinforced polymer strips produced with a novel bio-based thermoset polyester for structural strengthening. *Composites Science and Technology* **234**: 109936, 10.1016/j.compscitech.2023.109936.
60. Banerjee A, Jha K, Petru M *et al.* (2023) Fabrication and characterization of weld attributes in hot gas welding of alkali treated hybrid flax fiber and pine cone fibers reinforced poly-lactic acid (PLA) based biodegradable polymer composites: studies on mechanical and morphological properties. *Journal of Materials Research and Technology* **27**: 272–297, 10.1016/j.jmrt.2023.09.252.
61. Barczewski M, Matykiewicz D and Szostak M (2020) The effect of two-step surface treatment by hydrogen peroxide and silanization of flax/cotton fabrics on epoxy-based laminates thermomechanical properties and structure. *Journal of Materials Research and Technology* **9(6)**: 13813–13824, 10.1016/j.jmrt.2020.09.120.
62. Fakhreddini-Najafabadi S, Torabi M and Taheri-Behrooz F (2021) An investigation on the effects of synthesis on the mechanical properties of nanoclay/epoxy. *Journal of Materials Research and Technology* **15**: 5375–5395, 10.1016/j.jmrt.2021.10.129.
63. R E and G R (2024) Recent development and efficacy of wire mesh embedded natural fiber composite a review. *Results in Engineering* **24**: 103141, 10.1016/j.rineng.2024.103141.
64. Bouchareb N, Fellah M, Hezil N *et al.* (2024) Effect of milling time on structural, physical and photocatalytical properties of Ti-Ni alloy for biomedical applications. *The International Journal of Advanced Manufacturing Technology* **131(7–8)**: 3539–3553, 10.1007/s00170-024-13207-5.
65. Bouchareb N, Hezil N, Hamadi F and Fellah M (2024) Effect of milling time on structural, mechanical and tribological behavior of a newly developed Ti-Ni alloy for biomedical applications. *Materials Today Communications* **38**: 108201, 10.1016/j.mtcomm.2024.108201.
66. Dahmani M, Fellah M, Hezil N *et al.* (2023) Structural and mechanical evaluation of a new Ti-Nb-Mo alloy produced by high-energy ball milling with variable milling time for biomedical applications. *The International Journal of Advanced Manufacturing Technology* **129(11–12)**: 4971–4991, 10.1007/s00170-023-12650-0.
67. Farah M, Fellah M, Bouras D *et al.* (2024) Unraveling the role of sintering temperature on physical, structural and tribological characteristics of ball milled Co28Cr6Mo biomaterial based alloy. *Journal of Engineering Research* **12(3)**: 571–579, 10.1016/j.jer.2023.10.040.
68. Fellah M, Hezil N and Bouras D (2023) Structural, mechanical and tribological performance of a nano structured biomaterial Co–Cr–Mo alloy synthesized via mechanical alloying. *Journal of Materials Research and Technology* **25**: 2152–2165, 10.1016/j.jmrt.2023.06.031.
69. Rodríguez-Barajas N, Martin-Camacho UdJ and Salazar-Mendoza J (2024) PLGA/TI-ZN as nanocomposite for drug delivery of oleoresin. *Journal of Composites Science* **8(10)**: 431, 10.3390/jcs8100431.
70. Torres-Ramos MI, Martín-Camacho UdJ and Sánchez-Burgos JA (2024) CU2O nanoparticles as nanocarriers and its antibacterial efficacy. *Pharmaceuticals (Basel, Switzerland)* **17(9)**: 1124, 10.3390/ph17091124.
71. Lamiri L, Belgherbi O, Tounsi A *et al.* (2024) Eco-friendly electrodeposition sensing of hydrogen peroxide based on Co@Ag/PPy bimetallic nanohybrid. *Polymer Bulletin* **81(17)**: 16021–16042, 10.1007/s00289-024-05457-w.
72. Rodríguez-Barajas N, Ponce-Regalado MD, Segura-Almendárez MS *et al.* (2024) Plant-mediated synthesis and interaction of ZnO against breast and prostate cancer: review. *Results in Chemistry* **9**: 101654, 10.1016/j.rechem.2024.101654.
73. Chahmana S, Benghanem F, Fellah M *et al.* (2024) Integrated exploration of molecular structure, quantum chemical properties, molecular docking, and antioxidant activity of 4-(2-hydroxyanilino) pent-3-en-2-one. *Results in Chemistry* **8**: 101622, 10.1016/j.rechem.2024.101622.
74. Daoudi H, Bouafia A, Laouini SE *et al.* (2024) In vitro and in silico study of biosynthesized silver nanoparticles using nigella sativa extract against SARS-CoV-2 and Candida albicans. *Journal of Molecular Liquids* **405**: 125059, 10.1016/j.molliq.2024.125059.

How can you contribute?

To discuss this paper, please submit up to 500 words to the journal office at support@emerald.com. Your contribution will be forwarded to the author(s) for a reply and, if considered appropriate by the editor-in-chief, it will be published as a discussion in a future issue of the journal.

ICE Science journals rely entirely on contributions from the field of materials science and engineering. Information about how to submit your paper online is available at www.emeraldgrouppublishing.com/journal/jbibn, where you will also find detailed author guidelines.